A Non-Separable Two-Dimensional LWT for an Image Compression and Its Theoretical Analysis

Somchart Chokchaitam
Department of Electrical Engineering, Faculty of Engineering
Thammasat University, Pathum Thani 12121, Thailand
Phone 0-2564-3001 Ext. 3051, Fax 0-2564-3010 E-mail: csomchar@engr.tu.ac.th

Abstract

In this paper, we propose a new non-separable two-dimensional (2D) Lossless Wavelet Transform (LWT) for an image compression. Filter characteristics of our proposed 2D LWT are the same as those of 2D LWT based on applying two kinds of the conventional 1D LWT in horizontal and in vertical dimensions separately. However, coding performance of the proposed 2D LWT is better due to reduction of rounding effects. We theoretically analyze error in decoded image based on both 2D LWT to confirm an effectiveness of the proposed method. Both theoretical analysis and simulation results confirm the effectiveness of our proposed LWT in not only lossy coding but also lossless coding.

Key words: Lossless Wavelet Transform (LWT), non-separable two-dimensional, quantization, rounding effect, image compression

1. Introduction

Many researchers have been paying attention to image compression techniques [1] to reduce the number of bits required to represent image data. So far, we can generally classify image compression techniques into two types- lossy coding and lossless coding. These have been developed for a high compression ratio and a high quality of a decoded image, respectively.

Up to now, there have been many well-known coding standards introduced from the Joint Photographic Experts Group (JPEG) [2], JPEG, based on Discrete Cosine Transform (DCT) ([3], [4]), is the first standard for still image coding. This algorithm can provide high compression ratios; however, it is limited to only lossy coding. Then the lossless JPEG (L-JPEG) based on Differential Pulse Code Modulation (DPCM) [3] was proposed. The next standard was called JPEG-LS [5] based on a context-based modeling and a non-linear adaptive predictor referred to as Median Edge Detector (MED) in LOCO [6]. The compression ratio of JPEG-LS is better than the compression ration of L-JPEG since its filter coefficients are adaptive based on locally varying statistics from the image data. Unfortunately, both L-JPEG and JPEG-LS are not suitable for progressive resolution transmission because of the absence of the anti-aliasing filter, which can prevent aliasing occurring in low-resolution images.

Recently, JPEG-2000 [7] has been discussed as a new international compression standard that represents advances in image compression technique where the image coding system is optimized not only for efficiency, but also for scalability and interoperability in network and mobile environments. The Lossless Wavelet Transform (LWT) [7-9], constructed from lifting structures (LS) and rounding operations [10, 11], is selected as a key transform in JPEG-2000. However, the error generated from rounding operation [11] causes PSNR degradation in lossy coding when quantization is applied. Notice that the conventional LWT is a one-dimensional (1D) filter bank (FB) constructed from double LS. To perform 2D FB for image application, the 1D LWT is applied twice in horizontal and vertical dimensions, successively. Namely, it is "A Separable 2D LWT".

In this paper, we propose a non-separable two-dimensional (2D) LWT for an image compression. The number of rounding

operations of our proposed LWT is less than that of conventional 2D LWT, whereas filter characteristics of our proposed LWT are the same as those of conventional 2D LWT when error generated by the rounding operation is negligible. Coding performance of our proposed LWT is better than that of the conventional 2D LWT in lossy coding, especially at high bit rates when quantization errors are relatively small compared to the rounding errors.

This paper is organized as follows. We review signal processing of the conventional 2D LWT based on applying two kinds of the conventional 1D LWT in horizontal and vertical directions independently in section 2. Then, we propose a signal processing of a new non-separable 2D LWT for image compression in section 3. Theoretical analysis confirms advantages of our proposed 2D LWT in section 4. Simulation results confirm the effectiveness of our proposed method in both lossless coding and lossy coding in section 5. Finally, we summarize our proposed method in section 6.

2. The Conventional Two-Dimensional (2D) LWT

So far, many kinds of LWT have been proposed. Most of the LWT are one-dimensional (1D) LWT constructed from double lifting structures and rounding operations. In this paper, We renamed eight kinds of the LWT according to the numbers of taps in low-pass and high-pass filters as indicated in Table 1. The parameters $P_i(z)$ in i^{th} lifting structure of each LWT as shown in Table 1 are:

$$P_i(z) = \sum_{k=-3}^{3} a_{ki} z^k \qquad (1)$$

The conventional 2D LWT is constructed by applying two kinds of the conventional 1D LWT in horizontal and vertical directions independently as illustrated in figure 1. Input signal (X) is decomposed into 4 subbands (Y_{LL}, Y_{LH}, Y_{HL}, Y_{HH}). For example, Y_{LH} indicates horizontally low-passed and vertically high-passed subband. The z_1 and z_2 denotes horizontal and vertical dimension, respectively. The Q_{LL}, Q_{LH}, Q_{HL}, Q_{HH} denote quantization in subband LL, LH, HL, and HH, respectively. The LS denotes lifting structure. The ® and "↓2" denote the rounding operation and the down-sampler by two [12]. As shown in Fig. 1, six rounding operations are required to perform the conventional 2D LWT. We theoretically analyze errors in decoded image based on the conventional 2D LWT in section 4.

Table 1. Parameters of LWT [9].

LWT	i	a_{3i}	a_{2i}	a_{1i}	a_{0i}	a_{-1i}	a_{2i}	a_{-3i}
5/3	1	-	-	-1/2	-1/2	-	-	-
	2	-	-	-	1/4	1/4	-	-
13/11	1	-3/256	25/256	-150/256	-150/256	25/256	-3/256	-
	2	-	-	-	1/4	1/4	-	-
13/7-T	1	-	1/16	-9/16	-9/16	1/16	-	-
	2	-	-	-1/32	9/32	9/32	-1/32	-
13/3	1	-	-	-1/2	-1/2	-	-	-
	2	-	1/128	-5/128	9/32	9/32	-5/128	1/128
9/3-K	1	-	-	-1/2	-1/2	-	-	-
	2	-	-	1/256	63/256	63/256	1/256	-
9/3-S	1	-	-	-1/2	-1/2	-	-	-
	2	-	-	-3/64	19/64	19/64	-3/64	-
13/7-C	1	-	1/16	-9/16	-9/16	1/16	-	-
	2	-	-	-1/16	5/16	5/16	-1/16	
9/7-M	1	-	1/16	-9/16	-9/16	1/16	-	-
	2	-	-	-	1/4	1/4	-	-

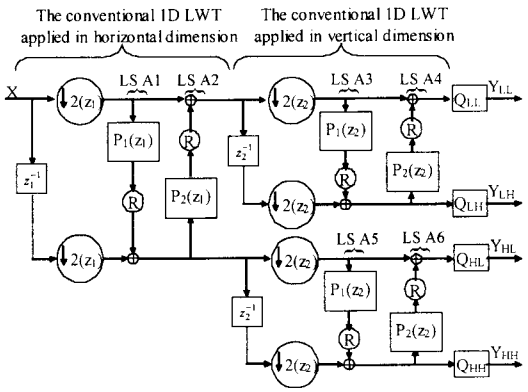

(a) Analysis part of the conventional 2D LWT.

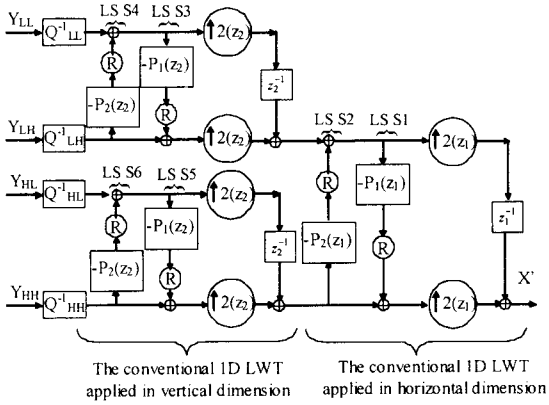

(b) Synthesis part of the conventional 2D LWT.

Fig.1 Signal processing of the conventional 2D LWT.

3. The proposed non-separable 2D LWT

In this paper, we propose the non-separable 2D LWT based on an objective to reduce numbers of rounding operations required in our proposed 2D LWT. Its filter characteristics are the same as those of the conventional 2D LWT. The signal processing of new non-separable 2D LWT is newly designed by applying two types of the conventional 1D LWT: LWT type 1 for a horizontal dimension and LWT type 2 for a vertical dimension. Notice that we have a freedom to select LWT type 1 and LWT type 2. They can be the same or different LWT.

As shown in figure 2, signal processing of our proposed 2D LWT requires only four rounding operations. The number of rounding operations required in our proposed 2D LWT is less because parameters in different LS of conventional 2D LWT can be combined. For an example, parameters of LS A1 and LS A5 in figure 1 are combined into those of LS A1' in figure 2. Parameters of LS A2 and LS A6 in figure 1 are combined into those of LS A2'. Therefore, the number of rounding operations required to perform the 2D LWT is reduced to four rounding operations.

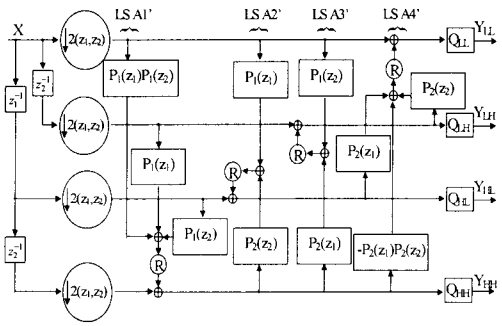

(a) Analysis part of the proposed 2D LWT.

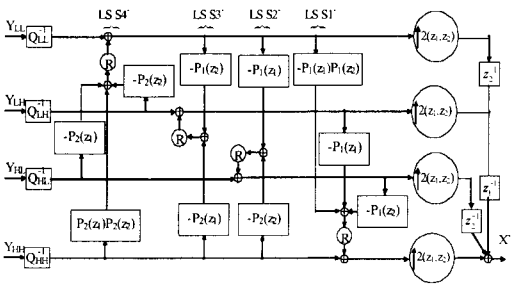

(b) Synthesis part of the proposed 2D LWT.

Fig. 2 Signal processing of the proposed non-separable 2D LWT

4. Theoretical Analysis

In this section, we theoretically illustrate advantages of the proposed non-separable 2D LWT. Theoretical analysis of the conventional 2D LWT and the proposed 2D LWT are illustrated in section 4.1 and section 4.2, respectively.

We analyze all signal processing in this paper based on the following assumptions. (1) All filters in this paper are linear and time-invariant filters, and (2) Correlations between each of the errors and the signals are zero (statistical independence). In this paper, we use z-transform expression defined by:

$$X(z) = \sum_{k=0}^{K-1} x(k) z^{-k} \tag{2}$$

where x(k) denotes signal's intensity. Value of x(k) for image signal is given as an "integer"

4.1 Theoretical analysis on the conventional 2D LWT

4.1.1 An equivalent expression of the conventional 2D LWT

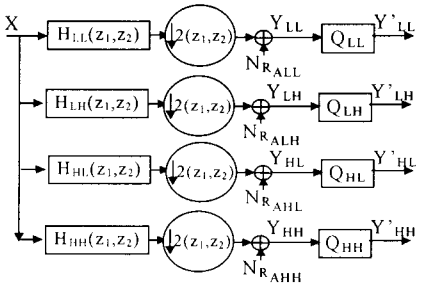

(a) An equivalent expression of analysis part of the 2D LWT.

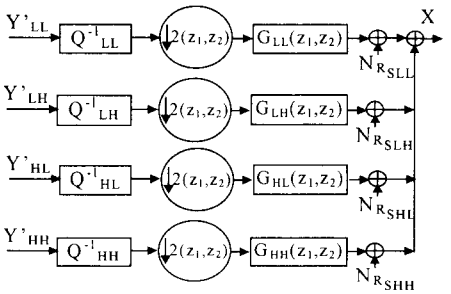

(b) An equivalent expression of Synthesis part of the 2D LWT.

Fig. 3. Equivalent expressions of the 2D LWTs.

Based on mentioned assumptions, signal processing in figure 1 can be replaced by its equivalent expression in figure 3 where its filter characteristics ($\mathbf{H_C}$ and $\mathbf{G_C}$) are:

$$\begin{bmatrix} \mathbf{H_{LLC}}(z_1,z_2) \\ \mathbf{H_{LHC}}(z_1,z_2) \\ \mathbf{H_{HLC}}(z_1,z_2) \\ \mathbf{H_{HHC}}(z_1,z_2) \end{bmatrix} = \mathbf{T_{C4}} * \mathbf{T_{C3}} * \mathbf{T_{C2}} * \mathbf{T_{C1}} * \begin{bmatrix} 1 \\ z_1^{-1} \\ z_2^{-1} \\ z_1^{-1}z_2^{-1} \end{bmatrix} \quad (3)$$

$$\begin{bmatrix} \mathbf{G_{LLC}}(z_1,z_2) \\ \mathbf{G_{LHC}}(z_1,z_2) \\ \mathbf{G_{HLC}}(z_1,z_2) \\ \mathbf{G_{HHC}}(z_1,z_2) \end{bmatrix} = \mathbf{T_{C1}^{-1}} * \mathbf{T_{C2}^{-1}} * \mathbf{T_{C3}^{-1}} * \mathbf{T_{C4}^{-1}} * \begin{bmatrix} z_1^{-1}z_2^{-1} \\ z_2^{-1} \\ z_1^{-1} \\ 1 \end{bmatrix}$$

where transform matrix ($\mathbf{T_{ci}}$ and $\mathbf{T^{-1}_{ci}}$) are based on parameters of the conventional 2D LWT in figure 1 as:

$$\mathbf{T_{C1}} = \begin{bmatrix} 1 & 0 & 0 & 0 \\ 0 & 1 & 0 & 0 \\ P_1(z_1^2) & 0 & 1 & 0 \\ 0 & P_1(z_1^2) & 0 & 1 \end{bmatrix}, \mathbf{T_{C1}^{-1}} = \begin{bmatrix} 1 & 0 & 0 & 0 \\ 0 & 1 & 0 & 0 \\ -P_1(z_1^2) & 0 & 1 & 0 \\ 0 & -P_1(z_1^2) & 0 & 1 \end{bmatrix} \quad (4)$$

$$\mathbf{T_{C2}} = \begin{bmatrix} 1 & 0 & P_2(z_1^2) & 0 \\ 0 & 1 & 0 & P_2(z_1^2) \\ 0 & 0 & 1 & 0 \\ 0 & 0 & 0 & 1 \end{bmatrix}, \mathbf{T_{C2}^{-1}} = \begin{bmatrix} 1 & 0 & -P_2(z_1^2) & 0 \\ 0 & 1 & 0 & -P_2(z_1^2) \\ 0 & 0 & 1 & 0 \\ 0 & 0 & 0 & 1 \end{bmatrix} \quad (5)$$

$$\mathbf{T_{C3}} = \begin{bmatrix} 1 & 0 & 0 & 0 \\ P_1(z_2^2) & 1 & 0 & 0 \\ 0 & 0 & 1 & 0 \\ 0 & 0 & P_1(z_2^2) & 1 \end{bmatrix}, \mathbf{T_{C3}^{-1}} = \begin{bmatrix} 1 & 0 & 0 & 0 \\ -P_1(z_2^2) & 1 & 0 & 0 \\ 0 & 0 & 1 & 0 \\ 0 & 0 & -P_1(z_2^2) & 1 \end{bmatrix} \quad (6)$$

$$\mathbf{T_{C4}} = \begin{bmatrix} 1 & P_2(z_2^2) & 0 & 0 \\ 0 & 1 & 0 & 0 \\ 0 & 0 & 1 & P_2(z_2^2) \\ 0 & 0 & 0 & 1 \end{bmatrix}, \mathbf{T_{C4}^{-1}} = \begin{bmatrix} 1 & -P_2(z_2^2) & 0 & 0 \\ 0 & 1 & 0 & 0 \\ 0 & 0 & 1 & -P_2(z_2^2) \\ 0 & 0 & 0 & 1 \end{bmatrix} \quad (7)$$

According to Reichel's paper [11], non-linearity of rounding operation generates additive noise and then the noise is propagated through FB to the reconstructed image. Therefore, rounding errors in its equivalent expression are:

$$\begin{bmatrix} N_{R_{S_{LLC}}}(z_1,z_2) \\ N_{R_{S_{LHC}}}(z_1,z_2) \\ N_{R_{S_{HLC}}}(z_1,z_2) \\ N_{R_{S_{HHC}}}(z_1,z_2) \end{bmatrix} = \begin{bmatrix} N_{R_{A4}}(z_1,z_2) \\ 0 \\ N_{R_{A6}}(z_1,z_2) \\ 0 \end{bmatrix} + \mathbf{T_{C4}} * \begin{bmatrix} 0 \\ N_{R_{A3}}(z_1,z_2) \\ 0 \\ N_{R_{A5}}(z_1,z_2) \end{bmatrix} \quad (8)$$

$$+ \mathbf{T_{C4}} * \mathbf{T_{C3}} * \begin{bmatrix} N_{R_{A2}}(z_1,z_2) \\ N_{R_{A2}}(z_1,z_2) \\ 0 \\ 0 \end{bmatrix} + \mathbf{T_{C4}} * \mathbf{T_{C3}} * \mathbf{T_{C2}} * \begin{bmatrix} 0 \\ 0 \\ N_{R_{A1}}(z_1,z_2) \\ N_{R_{A1}}(z_1,z_2) \end{bmatrix}$$

$$\begin{bmatrix} N_{R_{S_{LLL}}}(z_1,z_2) \\ N_{R_{S_{LHC}}}(z_1,z_2) \\ N_{R_{S_{HLC}}}(z_1,z_2) \\ N_{R_{S_{HHC}}}(z_1,z_2) \end{bmatrix} = \begin{bmatrix} 0 \\ 0 \\ N_{R_{S3}}(z_1,z_2) \\ N_{R_{S1}}(z_1,z_2) \end{bmatrix} + \mathbf{T_{C1}^{-1}} * \begin{bmatrix} N_{R_{S2}}(z_1,z_2) \\ N_{R_{S2}}(z_1,z_2) \\ 0 \\ 0 \end{bmatrix} \quad (9)$$

$$+ \mathbf{T_{C1}^{-1}} * \mathbf{T_{C2}^{-1}} * \begin{bmatrix} 0 \\ N_{R_{S5}}(z_1,z_2) \\ 0 \\ N_{R_{S5}}(z_1,z_2) \end{bmatrix} + \mathbf{T_{C1}^{-1}} * \mathbf{T_{C2}^{-1}} * \mathbf{T_{C3}^{-1}} * \begin{bmatrix} N_{R_{S4}}(z_1,z_2) \\ 0 \\ N_{R_{S6}}(z_1,z_2) \\ 0 \end{bmatrix}$$

where rounding errors N_{RAi} and N_{RSi} denote additive errors generated from rounding operation in lifting structure i[th] in figure 1 (a) and in figure 1 (b), respectively.

4.1.2 Error analysis in decoded image based on the conventional 2D LWT

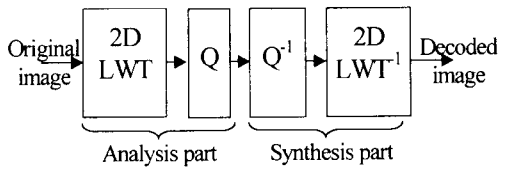

(a) The LWT-based coding system.

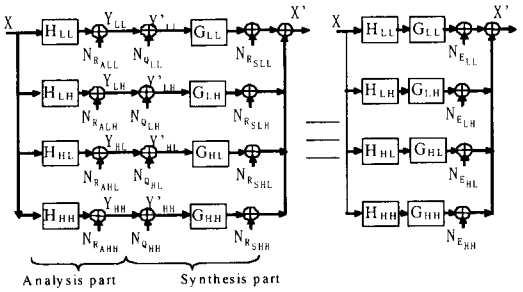

(b) An equivalent expression of the LWT-based coding system.

Fig. 4. The LWT-based coding system and its equivalent expression.

In this section, we theoretically analyze errors in decoded image of the conventional LWT-based coding systems as illustrated in figure 4. Errors in decoded image mainly generated from two sources: quantization and rounding operation. We can rewrite total error in each subband (N_E) from as:

$$\begin{bmatrix} N_{E_{LL,C}} \\ N_{E_{LH,C}} \\ N_{E_{HL,C}} \\ N_{E_{HH,C}} \end{bmatrix} = \begin{bmatrix} N_{Q_{LL}} \\ N_{Q_{LH}} \\ N_{Q_{HL}} \\ N_{Q_{HH}} \end{bmatrix} + \left(\begin{bmatrix} 0 \\ 0 \\ N_{R_{A1}} \\ N_{R_{A1}} \end{bmatrix} + \begin{bmatrix} 0 \\ 0 \\ N_{R_{S1}} \\ N_{R_{S1}} \end{bmatrix} \right) \quad (10)$$
$$+ \mathbf{T}_{C1}^{-1} * \left(\begin{bmatrix} N_{R_{A2}} \\ N_{R_{A2}} \\ 0 \\ 0 \end{bmatrix} + \begin{bmatrix} N_{R_{S2}} \\ N_{R_{S2}} \\ 0 \\ 0 \end{bmatrix} \right) + \mathbf{T}_{C1}^{-1} * \mathbf{T}_{C2}^{-1} * \left(\begin{bmatrix} 0 \\ N_{R_{A3}} \\ 0 \\ N_{R_{A5}} \end{bmatrix} + \begin{bmatrix} 0 \\ N_{R_{S3}} \\ 0 \\ N_{R_{S5}} \end{bmatrix} \right)$$
$$+ \mathbf{T}_{C1}^{-1} * \mathbf{T}_{C2}^{-1} * \mathbf{T}_{C3}^{-1} * \left(\begin{bmatrix} N_{R_{A4}} \\ 0 \\ N_{R_{A6}} \\ 0 \end{bmatrix} + \begin{bmatrix} N_{R_{S4}} \\ 0 \\ N_{R_{S6}} \\ 0 \end{bmatrix} \right)$$

We can approximate that both errors are independent, so the variance of errors (σ_E^2) in decoded image can be calculated from a variance of quantization error ($\sigma_{N_Q}^2$) and a variance of rounding error ($\sigma_{N_R}^2$) as:

$$\sigma_E^2 = \sigma_{N_Q}^2 + \sigma_{N_R}^2 \quad (11)$$

A variance of quantization error ($\sigma_{N_Q}^2$) is calculated from:

$$\sigma_{N_Q}^2 = \frac{1}{4}\left(\frac{\Delta_{LL}^2}{12}\|G_{LL}\|^2 + \frac{\Delta_{LH}^2}{12}\|G_{LH}\|^2 + \frac{\Delta_{HL}^2}{12}\|G_{HL}\|^2 + \frac{\Delta_{HH}^2}{12}\|G_{HH}\|^2\right) \quad (12)$$

where Δ denotes quantization step size and the norm $\|\mathbf{G}\|^2$ is defined as:

$$\|\mathbf{G}\|^2 = \sum_k g^2(k) \quad for\ G(z) = \sum_k g(k) z^{-k} \quad (13)$$

Next, we approximate a variance of rounding errors under assumption that if quantization is applied, the rounding errors in both analysis and synthesis part are independent. Therefore, a variance of rounding operation ($\sigma_{N_R}^2$) of the conventional 2D LWT based coding system is approximately calculated from:

$$\begin{aligned}\sigma_{N_{R,C}}^2 &= \frac{1}{2}(\sigma_{N_{RA1,C}}^2 + \sigma_{N_{RS1,C}}^2) + \frac{1}{2}(\sigma_{N_{RA2,C}}^2 + \sigma_{N_{RS2,C}}^2)\left\|1 - P_1(z_1^2)\right\|^2 \\ &+ \frac{1}{4}(\sigma_{N_{RA3,C}}^2 + \sigma_{N_{RS3,C}}^2)\left\|1 - P_1(z_2^2)\right\|^2 \\ &+ \frac{1}{4}(\sigma_{N_{RA4,C}}^2 + \sigma_{N_{RS4,C}}^2)\left\|1 - P_1(z_1^2)\right\|^2\left\|1 - P_1(z_2^2)\right\|^2 \\ &+ \frac{1}{4}(\sigma_{N_{RA5,C}}^2 + \sigma_{N_{RS1,C}}^2)\left\|1 - P_2(z_1^2) + P_1(z_1^2)P_2(z_1^2)\right\|^2 \\ &+ \frac{1}{4}(\sigma_{N_{RA6,C}}^2 + \sigma_{N_{RS6,C}}^2)\left\|1 - P_1(z_2^2)\right\|^2\left\|1 - P_2(z_1^2) + P_1(z_1^2)P_2(z_1^2)\right\|^2\end{aligned} \quad (14)$$

where $\sigma_{N_{R_A}}^2$ and $\sigma_{N_{R_S}}^2$ denote variances of rounding error in analysis part and in synthesis part, respectively. If we assume that power spectrum of all errors are flat, we can approximately calculate variance of rounding error from:

$$\sigma_{N_{RA1}}^2 = \ldots = \sigma_{N_{RA6}}^2 = \sigma_{N_{RS1}}^2 = \ldots = \sigma_{N_{RS6}}^2 = \frac{1}{12} \quad (15)$$

A variance of error generated from both quantization and rounding operations is theoretically calculated for eight kinds of LWT and compared to simulation results in the next section.

4.2 Theoretical analysis of the proposed non-separable 2D LWT

4.2.1 An equivalent expression of the proposed non-separable 2D LWT

Similarly, signal processing in figure 2 can be replaced by its equivalent expression in figure 3 where its filter characteristics ($\mathbf{H_P}$ and $\mathbf{G_P}$) are:

$$\begin{bmatrix} \mathbf{H}_{LLP}(z_1,z_2) \\ \mathbf{H}_{LHP}(z_1,z_2) \\ \mathbf{H}_{HLP}(z_1,z_2) \\ \mathbf{H}_{HHP}(z_1,z_2) \end{bmatrix} = \mathbf{T}_{P4} * \mathbf{T}_{P3} * \mathbf{T}_{P2} * \mathbf{T}_{P1} * \begin{bmatrix} 1 \\ z_1^{-1} \\ z_2^{-1} \\ z_1^{-1}z_2^{-1} \end{bmatrix} \quad (16)$$
$$\begin{bmatrix} \mathbf{G}_{LLP}(z_1,z_2) \\ \mathbf{G}_{LHP}(z_1,z_2) \\ \mathbf{G}_{HLP}(z_1,z_2) \\ \mathbf{G}_{HHP}(z_1,z_2) \end{bmatrix} = \mathbf{T}_{P1}^{-1} * \mathbf{T}_{P2}^{-1} * \mathbf{T}_{P3}^{-1} * \mathbf{T}_{P4}^{-1} * \begin{bmatrix} z_1^{-1}z_2^{-1} \\ z_2^{-1} \\ z_1^{-1} \\ 1 \end{bmatrix}$$

where transform matrix ($\mathbf{T_{pi}}$ and $\mathbf{T^{-1}_{pi}}$)) are based on parameters of non-separable 2D LWT in figure 2 as:

$$\mathbf{T}_{P1} = \begin{bmatrix} 1 & 0 & 0 & 0 \\ 0 & 1 & 0 & 0 \\ 0 & 0 & 1 & 0 \\ P_1(z_1^2)P_1(z_2^2) & P_1(z_1^2) & P_1(z_2^2) & 1 \end{bmatrix}, \quad (17)$$
$$\mathbf{T}_{P1}^{-1} = \begin{bmatrix} 1 & 0 & 0 & 0 \\ 0 & 1 & 0 & 0 \\ 0 & 0 & 1 & 0 \\ -P_1(z_1^2)P_1(z_2^2) & -P_1(z_1^2) & -P_1(z_2^2) & 1 \end{bmatrix}$$

$$\mathbf{T}_{P2} = \begin{bmatrix} 1 & 0 & 0 & 0 \\ 0 & 1 & 0 & 0 \\ P_1(z_1^2) & 0 & 1 & P_2(z_2^2) \\ 0 & 0 & 0 & 1 \end{bmatrix}, \mathbf{T}_{P2}^{-1} = \begin{bmatrix} 1 & 0 & 0 & 0 \\ 0 & 1 & 0 & 0 \\ -P_1(z_1^2) & 0 & 1 & -P_2(z_2^2) \\ 0 & 0 & 0 & 1 \end{bmatrix} \quad (18)$$

$$\mathbf{T}_{P3}=\begin{bmatrix}1&0&0&0\\P_1(z_2^2)&1&0&P_2(z_1^2)\\0&0&1&0\\0&0&0&1\end{bmatrix},\ \mathbf{T}_{P3}^{-1}=\begin{bmatrix}1&0&0&0\\-P_1(z_2^2)&1&0&-P_2(z_1^2)\\0&0&1&0\\0&0&0&1\end{bmatrix} \quad (19)$$

$$\mathbf{T}_{P4}=\begin{bmatrix}1&P_2(z_2^2)&P_2(z_1^2)&-P_2(z_2^2)P_2(z_1^2)\\0&1&0&0\\0&0&1&0\\0&0&0&1\end{bmatrix}$$

$$\mathbf{T}_{P4}^{-1}=\begin{bmatrix}1&-P_2(z_2^2)&-P_2(z_1^2)&P_2(z_2^2)P_2(z_1^2)\\0&1&0&0\\0&0&1&0\\0&0&0&1\end{bmatrix} \quad (20)$$

Eq. (3), and Eq. (16) confirm that filter characteristics of our proposed non-separable 2D LWT are the same as those of the conventional 2D LWT as:

$$\begin{bmatrix}\mathbf{H}_{LL,C}(z_1,z_2)\\\mathbf{H}_{LH,C}(z_1,z_2)\\\mathbf{H}_{HL,C}(z_1,z_2)\\\mathbf{H}_{HH,C}(z_1,z_2)\end{bmatrix}=\begin{bmatrix}\mathbf{H}_{LL,P}(z_1,z_2)\\\mathbf{H}_{LH,P}(z_1,z_2)\\\mathbf{H}_{HL,P}(z_1,z_2)\\\mathbf{H}_{HH,P}(z_1,z_2)\end{bmatrix},$$

$$\begin{bmatrix}\mathbf{G}_{LL,C}(z_1,z_2)\\\mathbf{G}_{LH,C}(z_1,z_2)\\\mathbf{G}_{HL,C}(z_1,z_2)\\\mathbf{G}_{HH,C}(z_1,z_2)\end{bmatrix}=\begin{bmatrix}\mathbf{G}_{LL,P}(z_1,z_2)\\\mathbf{G}_{LH,P}(z_1,z_2)\\\mathbf{G}_{HL,P}(z_1,z_2)\\\mathbf{G}_{HH,P}(z_1,z_2)\end{bmatrix} \quad (21)$$

Rounding errors in its equivalent expression are:

$$\begin{bmatrix}N_{R_{A,LL,P}}(z_1,z_2)\\N_{R_{A,LH,P}}(z_1,z_2)\\N_{R_{A,HL,P}}(z_1,z_2)\\N_{R_{A,HH,P}}(z_1,z_2)\end{bmatrix}=\begin{bmatrix}N'_{R_{A4}}(z_1,z_2)\\0\\0\\0\end{bmatrix}+\mathbf{T}_{P4}*\begin{bmatrix}0\\N'_{R_{A3}}(z_1,z_2)\\0\\0\end{bmatrix} \quad (22)$$

$$+\mathbf{T}_{P4}*\mathbf{T}_{P3}*\begin{bmatrix}0\\0\\N'_{R_{A2}}(z_1,z_2)\\0\end{bmatrix}+\mathbf{T}_{P4}*\mathbf{T}_{P3}*\mathbf{T}_{P2}*\begin{bmatrix}0\\0\\0\\N'_{R_{A1}}(z_1,z_2)\end{bmatrix}$$

$$\begin{bmatrix}N_{R_{S,LL,P}}(z_1,z_2)\\N_{R_{S,LH,P}}(z_1,z_2)\\N_{R_{S,HL,P}}(z_1,z_2)\\N_{R_{S,HH,P}}(z_1,z_2)\end{bmatrix}=\begin{bmatrix}0\\0\\0\\N'_{R_{S1}}(z_1,z_2)\end{bmatrix}+\mathbf{T}_{P1}^{-1}*\begin{bmatrix}0\\0\\N'_{R_{S2}}(z_1,z_2)\\0\end{bmatrix} \quad (23)$$

$$+\mathbf{T}_{P1}^{-1}*\mathbf{T}_{P2}^{-1}*\begin{bmatrix}0\\N'_{R_{S3}}(z_1,z_2)\\0\\0\end{bmatrix}+\mathbf{T}_{P1}^{-1}*\mathbf{T}_{P2}^{-1}*\mathbf{T}_{P3}^{-1}*\begin{bmatrix}N'_{R_{S4}}(z_1,z_2)\\0\\0\\0\end{bmatrix}$$

where rounding errors N'_{RAi} and N'_{RSi} denote errors generated from rounding operation in lifting the i^{th} structure in figure 2.

4.2.2 Error analysis in decoded image based on the proposed 2D LWT

Similarly, we analyze errors in decoded image of the conventional LWT-based coding systems as illustrated in figure 4. We can rewrite total error in each subband (N_E) as:

$$\begin{bmatrix}N_{E_{LL,P}}\\N_{E_{LH,P}}\\N_{E_{HL,P}}\\N_{E_{HH,P}}\end{bmatrix}=\begin{bmatrix}N_{Q_{LL}}\\N_{Q_{LH}}\\N_{Q_{HL}}\\N_{Q_{HH}}\end{bmatrix}+\left(\begin{bmatrix}0\\0\\0\\N'_{R_{A1}}\end{bmatrix}+\begin{bmatrix}0\\0\\0\\N'_{R_{S1}}\end{bmatrix}\right)$$

$$+\mathbf{T}_{P1}^{-1}*\left(\begin{bmatrix}0\\0\\N'_{R_{A2}}\\0\end{bmatrix}+\begin{bmatrix}0\\0\\N'_{R_{S2}}\\0\end{bmatrix}\right) \quad (24)$$

$$+\mathbf{T}_{P1}^{-1}*\mathbf{T}_{P2}^{-1}*\left(\begin{bmatrix}0\\N'_{R_{A3}}\\0\\0\end{bmatrix}+\begin{bmatrix}0\\N'_{R_{S3}}\\0\\0\end{bmatrix}\right)$$

$$+\mathbf{T}_{P1}^{-1}*\mathbf{T}_{P2}^{-1}*\mathbf{T}_{P3}^{-1}*\left(\begin{bmatrix}N'_{R_{A4}}\\0\\0\\0\end{bmatrix}+\begin{bmatrix}N'_{R_{S4}}\\0\\0\\0\end{bmatrix}\right)$$

Similarly, if quantization is applied for all subbands, we can calculate a variance of errors of the proposed LWT-based coding system from:

$$\sigma_{N_{R,P}}^2=\frac{1}{4}(\sigma_{N_{RA1,P}}^2+\sigma_{N_{RS1,P}}^2)+\frac{1}{4}(\sigma_{N_{RA2,P}}^2+\sigma_{N_{RS2,P}}^2)\left\|1-P_1(z_2^2)\right\|^2$$

$$+\frac{1}{4}(\sigma_{N_{RA3,P}}^2+\sigma_{N_{RS3,P}}^2)\left\|1-P_1(z_1^2)\right\|^2 \quad (25)$$

$$+\frac{1}{4}(\sigma_{N_{RA4,P}}^2+\sigma_{N_{RS4,P}}^2)\left\|1-P_1(z_1^2)\right\|^2\left\|1-P_1(z_2^2)\right\|^2$$

We can approximately calculate a variance of the errors by applying a variance of each rounding error in eq. (15). Table 2 theoretically confirms that a variance of rounding errors of the proposed 2D LWT less than that of the conventional 2D LWT.

Table 2. A variance of rounding error of the proposed 2D LWT and conventional 2D LWT.

LWT	$\sigma_{N_{R,C}}^2$	$\sigma_{N_{R,P}}^2$
5/3	0.439453	0.260417
13/11	0.491928	0.305102
13/7-T	0.472612	0.290532
13/3	0.438315	0.260417
9/3-K	0.439665	0.260417
9/3-S	0.438271	0.260417
13/7-C	0.471948	0.290532
9/7-M	0.474646	0.290532

5. Simulation results

In this section, we apply five standard images as input signals to illustrate effectiveness of our proposed method. Eight different kinds of the LWT [1] are applied as the conventional 1D LWT where their parameters are summarized in Table 1. Therefore, there are sixty-four possible kinds of proposed 2D LWT based on combination of eight kinds of the conventional 1D LWT. However, simulation results in this paper are based on the same LWT in both horizontal and vertical dimensions. Section 5.1 and Section 5.2 illustrate effectiveness of the proposed method in lossless coding and that in lossy coding, respectively. In this paper, the proposed 2D LWT and the conventional 2D LWT are applied only to one stage to confirm effectiveness of our proposed method.

5.1 An effectiveness in lossless coding

Table 3 and Table 4 illustrate lossless coding performance of both LWT in term of the entropy rate calculated by:

$$H = -\sum_{s} P_s \log_2 P_s \qquad (26)$$

where P_s indicates probability of a symbol "s". Table 3 and Table 4 indicate that entropy rates of the proposed method are slightly less than those of the conventional one.

Table 3. Entropy rate in lossless coding of the proposed LWT.

LWT	Aerial	Girl	Chest	Mobile	Barbara
5/3	5.9455	5.1415	6.4012	5.3538	5.5288
13/11	5.9197	5.1389	6.4483	5.3863	5.3844
13/7-T	5.9134	5.1257	6.424	5.3678	5.4077
13/3	5.9606	5.1452	6.4007	5.3581	5.5285
9/3-K	5.946	5.1431	6.4026	5.3538	5.532
9/3-S	5.9654	5.1473	6.4026	5.3608	5.5302
13/7-C	5.9216	5.1264	6.4245	5.37	5.408
9/7-M	5.9085	5.1279	6.4295	5.3706	5.4139

Table 4. Entropy rate in lossless coding of the conventional LWT.

LWT	Aerial	Girl	Chest	Mobile	Barbara
5/3	5.9457	5.1447	6.4008	5.3544	5.5302
13/11	5.921	5.1401	6.4484	5.3873	5.3882
13/7-T	5.9145	5.1288	6.4244	5.3688	5.4138
13/3	5.9571	5.1475	6.4007	5.3583	5.5291
9/3-K	5.9435	5.1443	6.4022	5.3537	5.5318
9/3-S	5.9619	5.1501	6.4013	5.3602	5.5298
13/7-C	5.9231	5.1311	6.4248	5.371	5.4143
9/7-M	5.9105	5.1315	6.4306	5.3716	5.4179

5.2 An effectiveness in lossy coding

Table 5-12 illustrate lossy coding performance of both methods in term of PSNR (Peak Signal to Noise Ratio) defined as

$$PSNR = 10\log_{10}\left(\frac{255^2}{\sigma_E^2}\right) \quad [dB] \qquad (27)$$

where σ_E^2 denotes variance of error signal between original signal and decoded signal. The "proposed" and "conventional" indicate "proposed non-separable 2D LWT" and "the conventional 2D LWT", respectively. To be comparable to a conventional quantization, quantization step size for all is set in the same value. Table 5-12 practically confirms that coding performance of the proposed 2D LWT is better than that of the conventional 2D LWT. Moreover, Table 5-12 confirms that theoretical analysis is accurate to predict PSNR of the decoded image. Fig. 5 illustrates rate distortion curve of "Barbara" based on the "5/3". Fig. 5 also confirms that coding performance of the proposed 2D LWT is always better than that of the conventional 2D LWT; especially in high bit rates. Notice that coding performance of the proposed one is slightly better than that of the conventional one at a low bit rate. Fig. 6 illustrates an original image "Barbara". Fig. 7 and Fig. 8 illustrate decoded images at total bit rate = 5 bpp generated from our proposed 2D LWT and that from the conventional one, respectively.

Table 5. PSNR of decoded image based on the "5/3" LWT (simulation/theoretical).

Image Name	Conventional		Proposed	
	5 bpp.	4 bpp.	5 bpp.	4 bpp.
Aerial	48.2/48.4	44.6/44.8	49.0/49.3	44.9/45.2
Girl	49.8/49.7	47.7/47.8	49.8/50.9	48.4/48.6
Chest	46.3/46.2	42.5/42.8	46.6/46.7	42.7/43.0
Mobile	48.5/49.3	46.9/47.2	48.7/50.4	47.2/47.9
Barbara	48.3/49.4	46.0/46.4	48.7/50.5	46.4/47.0

Table 6. PSNR of decoded image based on the "13/11" LWT (simulation/theoretical).

Image Name	Conventional		Proposed	
	5 bpp.	4 bpp.	5 bpp.	4 bpp.
Aerial	47.8/47.9	44.4/44.2	48.2/48.7	44.6/44.6
Girl	49.0/49.2	47.2/47.3	49.2/50.3	47.5/48.0
Chest	45.2/45.7	41.8/42.2	45.5/46.2	42.0/42.5
Mobile	47.6/48.7	45.9/46.7	48.1/49.8	46.4/47.3
Barbara	48.4/48.8	45.8/45.9	48.7/49.9	46.4/46.4

Table 7. PSNR of decoded image based on the "13/7-T" LWT (simulation/theoretical).

Image Name	Conventional		Proposed	
	5 bpp.	4 bpp.	5 bpp.	4 bpp.
Aerial	47.8/48.1	44.5/44.5	48.3/49.0	44.8/44.8
Girl	49.1/49.4	47.2/47.5	49.4/50.6	47.7/48.2
Chest	45.6/45.9	42.0/42.5	46.0/46.4	42.2/42.7
Mobile	47.8/48.9	46.1/46.9	48.3/50.0	46.6/47.5
Barbara	48.5/49.1	45.9/46.1	48.8/50.2	46.3/46.6

Table 8. PSNR of decoded image based on the "13/3" LWT (simulation/theoretical).

Image Name	Conventional		Proposed	
	5 bpp.	4 bpp.	5 bpp.	4 bpp.
Aerial	48.0/48.4	44.6/44.8	48.5/49.4	44.8/45.2
Girl	49.6/49.7	47.6/47.8	49.8/51.0	47.9/48.6
Chest	46.4/46.2	42.5/42.8	46.6/46.8	42.7/43.0
Mobile	48.3/49.3	46.8/47.2	48.7/50.4	47.2/47.9
Barbara	48.3/49.4	46.0/46.4	48.7/50.6	46.2/47.0

Table 9. PSNR of decoded image based on the "9/3-K" LWT (simulation/theoretical).

Image Name	Conventional		Proposed	
	5 bpp.	4 bpp.	5 bpp.	4 bpp.
Aerial	48.3/48.4	44.6/44.8	48.7/49.3	44.8/45.1
Girl	49.8/49.7	47.5/47.8	49.7/50.9	48.0/48.6
Chest	46.3/46.2	42.5/42.8	46.6/46.7	42.6/43.0
Mobile	48.4/49.3	46.8/47.2	48.7/50.4	47.2/47.9
Barbara	48.2/49.4	45.9/46.4	48.6/50.5	46.1/46.9

Table 10. PSNR of decoded image based on the "9/3-S" LWT (simulation/theoretical).

Image Name	Conventional		Proposed	
	5 bpp.	4 bpp.	5 bpp.	4 bpp.
Aerial	48.0/48.4	44.6/44.8	48.5/49.4	44.9/45.2
Girl	49.7/49.7	47.6/47.8	49.8/51.0	48.1/48.6
Chest	46.4/46.2	42.5/42.8	46.7/46.8	42.7/43.1
Mobile	48.2/49.3	46.9/47.2	48.6/50.4	47.3/47.9
Barbara	48.3/49.4	46.0/46.4	48.7/50.6	46.1/47.0

Table 11. PSNR of decoded image based on the "13/7-C" LWT (simulation/theoretical).

Image Name	Conventional		Proposed	
	5 bpp.	4 bpp.	5 bpp.	4 bpp.
Aerial	47.8/48.1	44.6/44.5	48.4/49.0	44.9/44.9
Girl	49.0/49.4	47.2/47.5	49.3/50.3	47.7/48.2
Chest	45.5/45.9	42.0/42.5	46.0/46.4	42.2/42.7
Mobile	47.8/49.0	46.2/46.9	48.4/50.0	46.6/47.5
Barbara	48.4/49.1	45.9/46.1	48.9/50.2	46.3/46.6

Table 12. PSNR of decoded image based on the "9/7-M" LWT (simulation/theoretical).

Image Name	Conventional		Proposed	
	5 bpp.	4 bpp.	5 bpp.	4 bpp.
Aerial	48.0/48.1	44.5/44.4	48.3/48.9	44.8/44.8
Girl	49.2/49.3	47.3/47.4	49.4/50.5	47.7/48.2
Chest	45.5/45.9	42.0/42.4	45.9/46.4	42.1/42.6
Mobile	47.9/48.9	46.1/46.8	48.4/50.0	46.5/47.5
Barbara	48.5/49.0	45.9/46.0	48.8/50.1	46.2/46.6

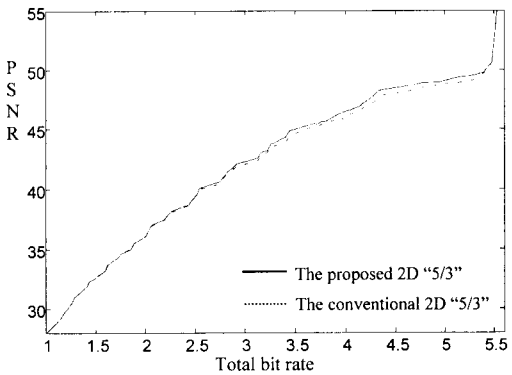

Fig. 5 Rate distortion curve of "Barbara" based on "5/3".

Fig. 6 An original image "Barbara".

Fig. 7 A decoded image "Barbara" based on our proposed 2D "5/3" at total bit rate = 5 bpp., PSNR = 48.7 dB.

Fig. 8 A decoded image "Barbara" based on the conventional 2D "5/3" at total bit rate = 5 bpp., PSNR = 48. 3 dB.

6. Conclusion

In this paper, we proposed a new non-separable 2D LWT with fewer rounding operations. The coding performance of our proposed method is better than that of the conventional 2D LWT because the proposed LWT has less number of rounding operations required in 2D filter bank, however filter characteristics of both methods are exactly the same. Simulation results confirm effectiveness of our proposed method in lossy coding at high bit-rates, additionally in lossless coding.

Computational load of the proposed non-separable 2D LWT is increased, compared to that of the conventional one.

7. Acknowledgements

The author would like to thank Faculty of Engineering, Thammasat University, Thailand for financial support this work.

8. References

[1] K. R. Rao and J. J. Hwang, Technique and Standards for Image, Video and Audio Coding, Prentice Hall, Inc. 1996.

[2] JPEG CD10918-1, Digital Compression Coding of Continuous-tone Still Images, JPEG-9-R6, Jan.1991.

[3] N. S. Jayant and P. Noll, Digital Coding of Wave Forms, Englewood Cliffs, NJ: Prentice-Hall, 1984.

[4] K. R. Rao and P. Yip, Discrete Cosine Transform Algorithms, Advantages, Applications, Academics Press, Inc., 1990.

[5] ISO/IEC FCD14495, Lossless and Near-lossless Coding of Continuous-tone Still Image (JPEG-LS), 1997.

[6] M. J. Weinberger, G. Seroussi, G. Sapiro, LOCO-I: A Low Complexity, Context-based, Lossless Image Compression Algorithm, IEEE Computer Society Press, Mar.1996.

[7] M. Rabbani and R. Joshi, An Overview of the JPEG 2000 Still Image Compression Standard, IEEE Trans. on Signal Processing: Image Communication, Vol. 17, pp. 3-48, 2002.

[8] S. Chokchaitam, M. Iwahashi, P. Zavarsky, N. Kambayashi, Lossless Coding Gain and Its Application to Evaluation of Lossless Wavelets, IEEE ISPACS'00, Nov. 2000.

[9] S. Chokchaitam, and M. Iwahashi, Performance Evaluation of the Lossless/Lossy Wavelet for Image Compression under Lossless/Lossy Coding Gain, IEICE Special Section on Digital Signal Processing, Vol. E85-A, No. 8, pp. 1882-1891, Aug. 2002.

[10] W. Sweldens, The Lifting Scheme: A Construction of Second Generation Wavelets, Tech. Rep. 1995:6, Industrial Math. Initiative, Dept. of Math., Univ. of South Carolina, 1995.

[11] J. Reichel, G. Menegaz, M. J. Nadenau, M. Kunt, Integer Wavelet Transform for Embedded Lossy to Lossless Image Compression, IEEE Trans. On Image Processing, Vol. 10, No. 3, pp. 383-392, March 2001.

[12] P. P. Vaidyanathan, Multirate Systems and Filter Banks, Prentice Hall Signal Processing Series, 1993.